ICAS 2021 SHANG HAI
International Council of the Aeronautical Sciences
32nd Congress of the International Council of the Aeronautical Sciences
September 6-10, 2021 Pudong Shangri-La, Shanghai, China

WIND-TUNNEL INVESTIGATION OF COMMERCIAL TRANSPORT AIRCRAFT STATIC AND DYNAMIC AERODYNAMIC CHARACTERISTICS AT EXTREME FLIGHT CONDITIONS

ZHANG Lei[1,2], LIU Zhitao[2], CEN Fei[2], JIANG Yong[2] , SUN Haisheng[2],

[1] School of Aeronautic Science and Engineering, Beihang University, Beijing 100191, China
[2] Low Speed Aerodynamic Institute, China Aerodynamic Research and Development Center, Mianyang 621000, China

Abstract

Extreme flight conditions are closely related to flight safety for commercial transport aircraft. A series of static and dynamic wind tunnel tests cover high angle of attack/sideslip using a commercial transport aircraft were conducted at Chinese Aerodynamics Research and Development Center (CARDC) to study the aerodynamic characteristics for this kind of configuration. The results show that the aerodynamic characteristics at high angle of attack/sideslip differ a lot from that in normal flight envelop. It is necessary to acquire high fidelity data under extreme flight conditions. This database can be used for the study of the aerodynamic modeling and flight simulation technology.

Keywords: commercial transport aircraft, wind tunnel test, extreme flight condition, aerodynamic characteristic

1. Introduction

One of the most important characteristics for large transport aircraft is flying safety. Statistics show that 'Loss of Control-In Flight' (LOC-I) is one of the major important factors in serious flight accidents for commercial transport aircraft [1]. Fall into extreme flight condition by accident and fail to recovery is the important reason that cause LOC-I [2].

Aircraft in extreme flight conditions involve in large angle of attack, sideslip and angular velocity, which is far beyond normal flight envelope. Aerodynamic characteristics in these conditions often acquired from estimation or extrapolation from wind tunnel database for the reason that the flight envelop of this kind configuration is relatively small, there is no requirement to get high fidelity data in this region generally.

Flight accidents have demonstrated that aircraft can easily reach extreme flight conditions in some cases. Current database is not sufficient for flying simulation and plot training, and also difficult to validate in flying test [3].

In order to get high-fidelity aerodynamic characteristics in extreme flight conditions for commercial transport airplane, a series wind tunnel tests were conducted and many meaningful aerodynamic characteristics were acquired.

2. Test Description

2.1 Test Model

The Common Research Model (CRM) used for research is a conventional commercial transport configuration with two engines under the wing (Figure1), which was publish by NASA. The model used for test is made of fiber with a scale of 2.45%. Surfaces contain rudder, elevator, stabilizer and aileron. More geometry information is presented in table1.

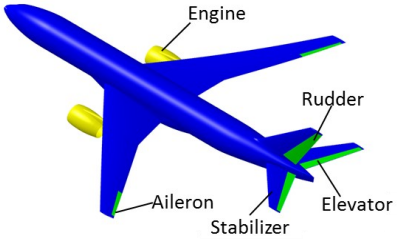

Figure 1 – Common research model

Table 1. Geometry properties of the model

Parameter	CRM
Wing span b (m)	1.436
Mean aerodynamic chord c_A (m)	0.171
Wing area S (m^2)	0.2292

2.2 Test Content

Both static and forced oscillation tests were conducted in the FL-14(Φ3.2m) wind tunnel using the same model. The model was supported by single degree of freedom dynamic test device.

All the static and the rolling oscillation tests were carried out by tail support while belly support were used for pitch and yaw oscillation tests. The model installation is illustrated in figures 2a-b. Six-component data were acquired by an internal strain-gauge balance installed inside the fuselage.

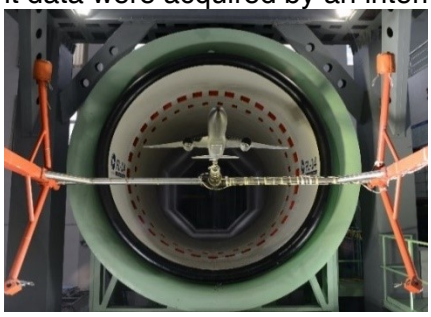

Figure 2a – Model set-up; tail support

Figure 2b – Model set-up; belly support

The wind speed of static tests was 35m/s, while the dynamic tests were carried out at 30 m/s, corresponding to the Reynolds number based on mean aerodynamic chord is 3.5×10^5 and 3.0×10^5, respectively. Static results were acquired at the angle of attack from -10° to 80°, while the sideslip from -30° to 30°. Benefiting from the continuous scanning technology, six-component data were output at intervals of 0.5°. As for the forced oscillation tests, the angle of attack is from -10° to 60°.

Basic aerodynamics characteristics, control power of surfaces was researched in static tests. The damping characteristics of three degrees of freedom were mainly studied in forced oscillation tests. The model was oscillated in sinusoidal motion with different amplitudes and frequencies individually in pitch, roll and yaw body axis.

In addition, circular boundary layer transition bands were fixed at 10% of the leading edge of the wing, stabilizer and vertical tail to reduce the influence of Reynolds Number. The model contains all the control surfaces and two nacelles in the tests. All the control surfaces deflection are 0° by default and sign conventions are placed in table2.

Table 2 Control surface sign conventions of the model

Stabilizer	Positive Trailing Edge Down
Elevator	Positive Trailing Edge Down
Rudder	Positive Trailing Edge Down
Aileron	Right Wing Positive Trailing Edge Down Left Wing Positive Trailing Edge Up

3. Typical Results

Configuration like CRM has similar aerodynamic characteristics under extreme flight conditions [3],

the values of vertical axes are absent in the charts so the results could be better to represent this kind of configuration. Some of the charts also contain 'Nominal Simulation Extrapolation' (NSE) curves to show the traditional method to get aerodynamic characteristics where the values are held constant as the angle of attack/sideslip beyond normal envelope.

3.1 Longitudinal Aerodynamics and Stability

The longitudinal aerodynamics and stability were put in Figures 3a-d, the effect of stabilizer was also taken into account while other control surfaces are zero. It can be seen from Figure 3a that the stall appears around 10°, the critical angle is about 15° and the maximum lift coefficient can be reached at around 35°.

In Figure 3b, the maximum trim angle of attack can reach 34° when stabilizer is -18°. Although it cannot be used for trimming when stabilizer is 7°, it can be used to provide pitch moment under extreme conditions such as elevator failure. When the angle of attack approaches and exceeds the critical angle, the non-linearity of pitch moment increases significantly and the pitch stability decreases into neutral or even unstable.

The NSE lines are also shown in Figure 3b while the angle of attack is beyond α=30°. It differs a lot from the wind tunnel results, the NSE curves tend to have a constant pitch moment rather than strong nonlinearity test results. As a result, applying the NSE results to aerodynamic modeling will reduce the modeling accuracy.

The effect of sideslip for basic longitudinal characteristics were shown in Figures 3c-d. As the sideslip and angle attack increases, both the lift and pitch moment slightly decline as α and β go up and there is no sudden change.

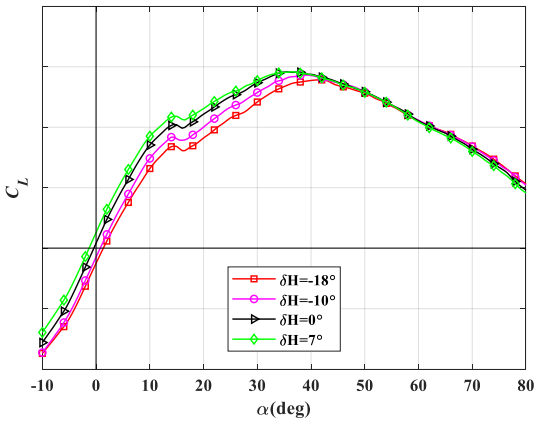

Figure 3a – Longitudinal characteristics and stabilizer effect, CL-α

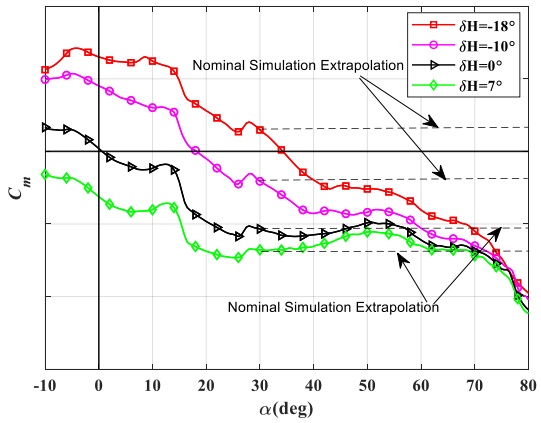

Figure 3b – Longitudinal characteristics and stabilizer effect, Cm-α

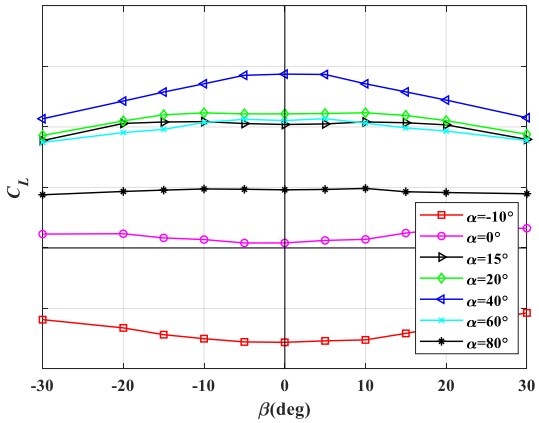

Figure 3c – Longitudinal characteristics, CL-β

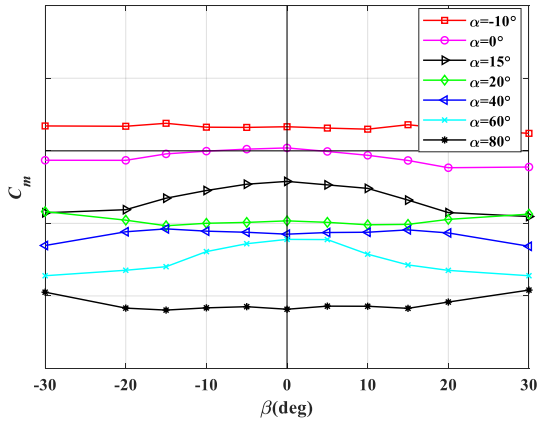

Figure 3d – Longitudinal characteristics, Cm-β

3.2 Lateral/Directional Aerodynamics and Stability

The lateral aerodynamic characteristics are shown in Figures 4a-b and the vertical axes values are the same in two figures. The lateral stability of the aircraft drops sharply over stall angle and stay neutral when the angles of attack are 20° -26°. As angle of attack and sideslip increases, the lateral stability gradually recovers. Given the low slop of the curve in small angle of attack and large sideslip (Figure 4b), it is likely to be longitudinally unstable in this situation.

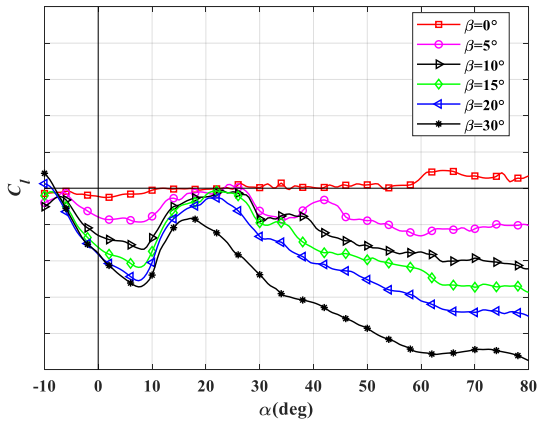

Figure 4a – Lateral characteristics; Cl-α

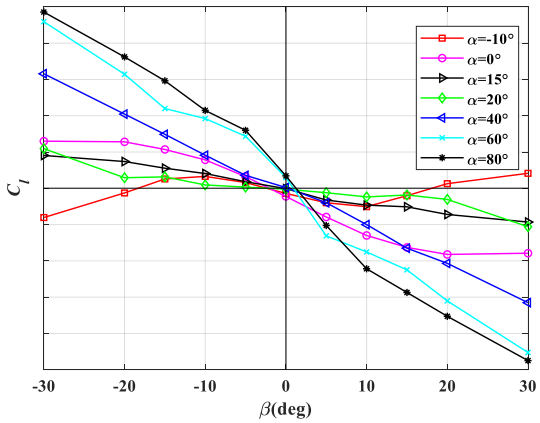

Figure 4b – Lateral characteristics; Cl-β

The directional aerodynamic characteristics are shown in Figures 5a-b. Also, the vertical values of two charts are the same. In addition, Figure 5a illustrates the result without vertical tail where the sideslip angle is 30°. As vertical tail produces majority of directional control power, the airflow on vertical tail begins to separate when the sideslip is greater than β=15° before the stall angle of attack, resulting the decrease in directional stability.

The reason why the directional stability increases at α=25° when β=30° is that the vertical tail is already outside the wake of the wing and the body (Figure 5a), The vertical tail control power almost lost as the value of yaw moment is almost the same as the line with no vertical tail when the angle of attack is greater than 62°. Furthermore, directional stability continuously decreases and even become unstable (Figure 5b) as the angle of attack is over 40°.

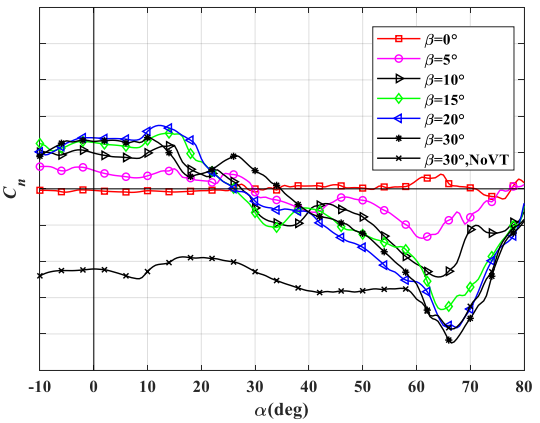

Figure 5a – Directional characteristics Cn-α

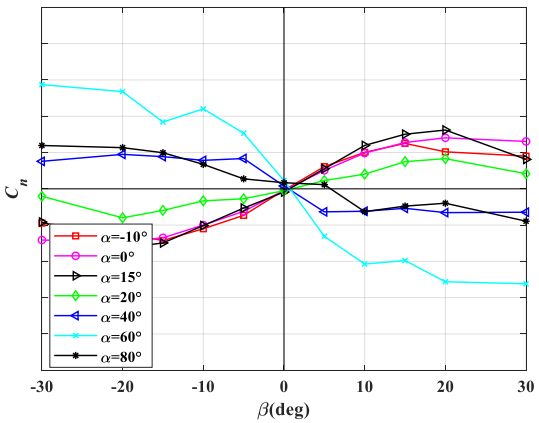

Figure 5b – Directional characteristics Cn-β

3.3 Longitudinal Control Power

Longitudinal control power is shown in Figures 6a-b. The deflection range of the elevator is -35° to 30°. Elevator efficiency is basically linear along with the surface deflection at small angle of attack, the control power gradually declines when angle of attack is over stall and reaches to zero when elevator deflection is greater than 10° at high α.

Figure 6b also shows the NSE line when angle of attack is over 30°. It can be found that the elevator control power acquired from wind tunnel tests is much smaller than the result of simulation

extrapolation. Applying NSE result in post-stall state to aerodynamic modeling will bring great modeling deviation which cannot reflect the real aerodynamic characteristics.

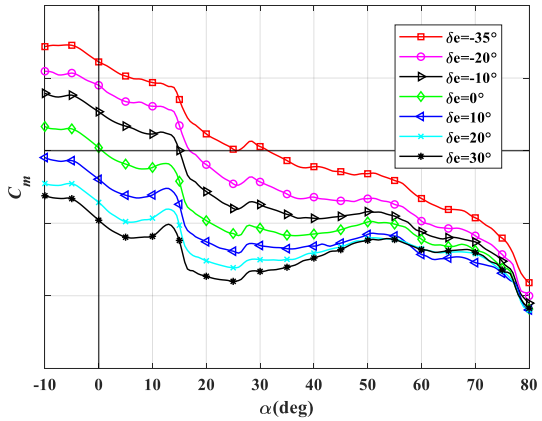

Figure 6a – Elevator control power; stabilizer zero

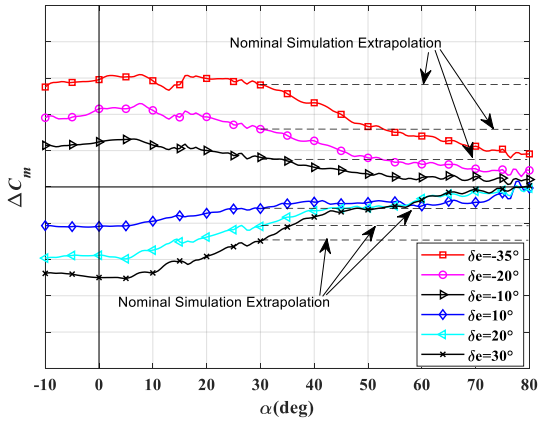

Figure 6b – Incremental elevator control power; stabilizer zero

3.4 Lateral/Directional Control Power

The lateral control power is shown in Figures 7a-b. The left and right aileron deflected at the same time during the test. Given its small value, range of vertical axes in pictures has been enlarged in order to observe the results.

It is clear that the aileron control power keeps at high level in small angle of attack and drops rapidly after stall occurs and remains relatively stable before α=25°. After that, it keeps fluctuating till α=80°. Since the small change in aileron control power after stall, the NSE line is consistent with the test results. Roll control power does not change a lot as the sideslip goes up, which can be seen from Figure 7b.

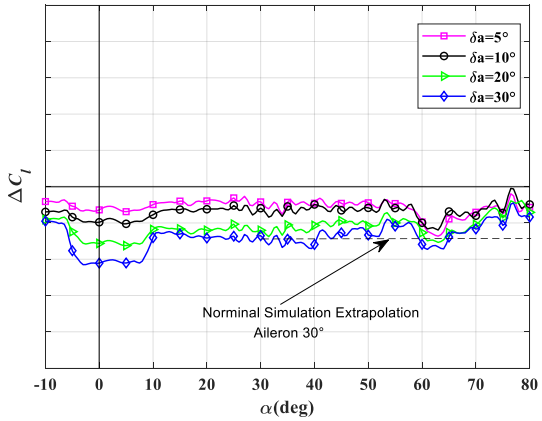

Figure 7a – Incremental aileron control power; β=0°

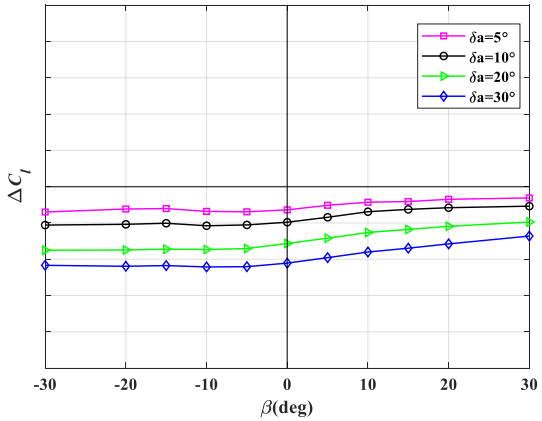

Figure 7b – Incremental aileron control power; sideslip effect; α=0°

Rudder control power under different angle of attack and sideslip are illustrated in Figures 8a-b. It keeps stable when the rudder angle is less than 30° before stall. When the angle of attack is greater than 55°, rudder control power almost lost. Figure 8a also shows that the control power of the test is smaller than NSE result especially at high angle of attack.

Regarding the influence of sideslip angle, Figure 8b witnesses a higher control power as the direction of rudder and the sideslip angle are the same at large rudder angle. This is because that the power loss mainly comes from the stall on vertical tail, much greater the angle between the rudder and the airflow, more serious the stall happenss on vertical in large sideslip, which cause more control power loss under this condition.

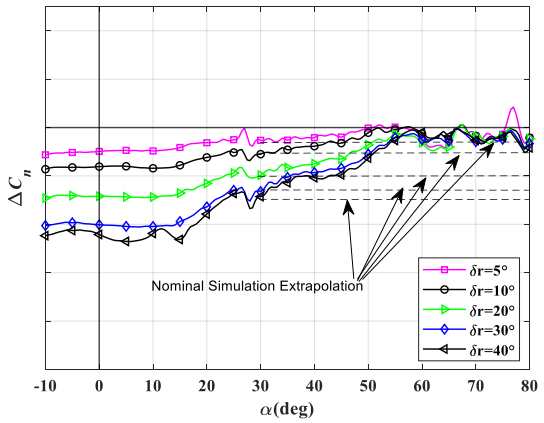

Figure 8a – Incremental rudder control power; β=0°

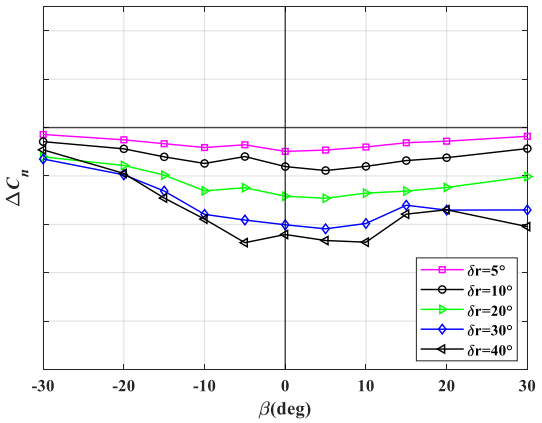

Figure 8b – Incremental elevator control power; sideslip effect; α=0°

3.5 Longitudinal Damping Characteristics

The longitudinal damping characteristics obtained from pitch oscillation are shown in Figures 9a-b.

Figure 9a illustrates the result in different oscillation frequency. NSE line is also shown in Figure 9b where the amplitude effect is mainly studied. The longitudinal damping characteristic of the model almost hold constant before stall.

As oscillation frequency decreases, damping characteristic gradually changes from stable to unstable at 15°. When the angle of attack is from 8° to 32°, the pitch damping first drops sharply to unstable and then returns to the value before stall at last. It means that the unsteady aerodynamic characteristics are significantly enhanced in this interval, which differ a lot from that before stall. Similar phenomena can also be seen in Figure 9b where the results are mainly affected by amplitude. NSE line in the chart almost holds constant and cannot reflect the real pitch damping characteristics from 8° to 32°.

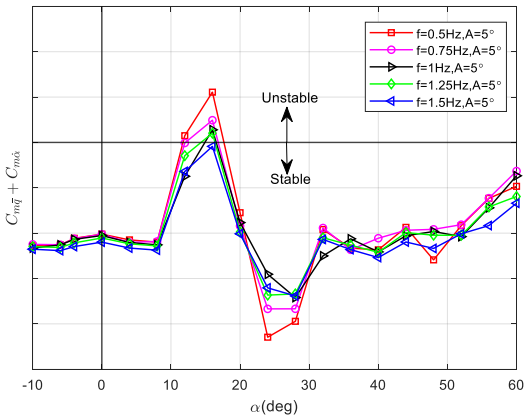

Figure 9a – Pitch damping characteristics; frequency effect

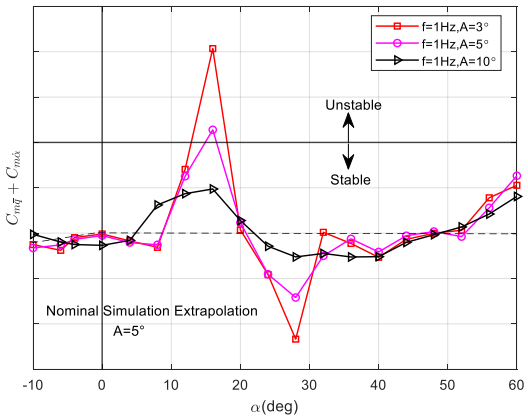

Figure 9b –Pitch damping characteristics; damping characteristics; amplitude effect

3.6 Lateral/Directional Damping Characteristics

Roll and yaw damping characteristics are listed in Figures 10a-b and 11a-b respectively. The magnitude is much smaller compared with pitch dynamic stability derivatives.

Oscillation frequency and amplitude have a small effect on the roll derivatives before the stall angle (Figure 10a-b). Although the pitch damping magnitude varies, the roll damping characteristics remain stable. Both two charts witness a slow increase in roll damping at first and then slow diminish and finally, return to stable when the angles of attack between 12°-46°. Frequency and amplitude of oscillation have impact on test result and change the damping characteristics at 30°-45°. The NSE

curve (Fig10b) overestimates the roll damping characteristic over the entire angle of attack.

Directional damping characteristics does not change too much along with amplitude and frequency and remain stable when the angle of attack is less than 24° (Figure 11a-b). It reaches a peak at 28° and the sign becomes positive, which means yaw damping characteristic reversed and becomes unstable. Although NSE curve (Figure 11b) captures the yaw damping characteristics in most angles of attack, it loses some key damping information at certain angles.

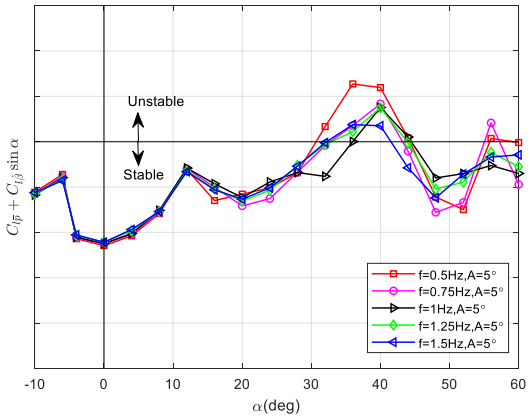

Figure 10a – Roll damping characteristics; frequency effect

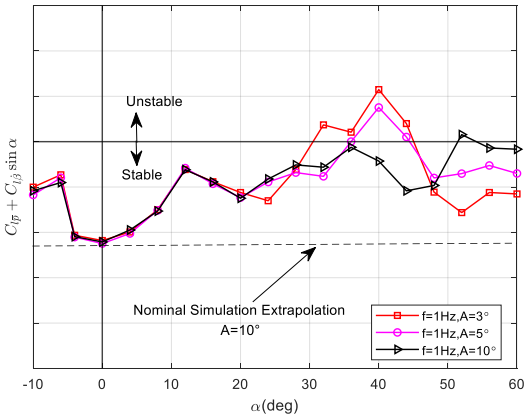

Figure 10b – Roll damping characteristics; amplitude effect

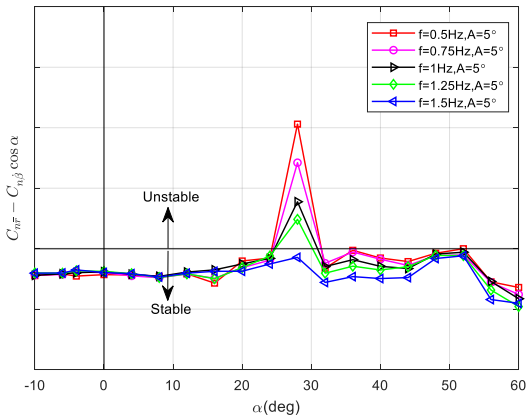

Figure 11a – Yaw damping characteristics; frequency effect

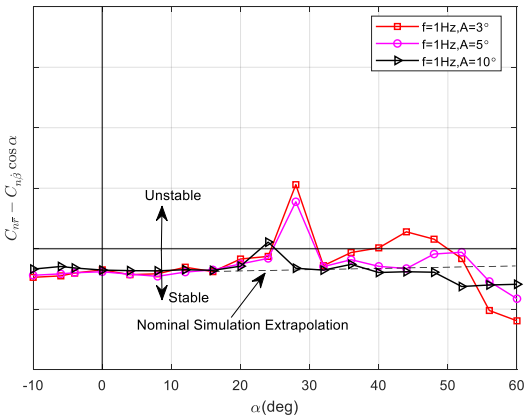

Figure 11b –Yaw damping characteristics; amplitude effect

4. Conclusions

The static and dynamic aerodynamic characteristics of commercial transport aircraft under extreme flight conditions have strong nonlinearity and unsteadiness. The pitch and yaw stability are greatly decreased or even unstable at high angles of attack and large sideslip while roll stability decreases severely at medium and large angles of attack and recover at higher angle of attack. Control power of elevator and rudder decline as angle of attack go up. Oscillation frequency and amplitude have influence on the test results, damping characteristics decline and even become unstable at certain angles after stall.

Nominal Simulation Extrapolation (NSE) method cannot reflect the real aerodynamic characteristics of the aircraft under extreme flight conditions in some cases. On the one hand, the estimation is relatively conservative, the elevator and rudder control power and rolling damping characteristics obtained from NSE are higher than test results. On the other hand, NSE method may lose some key aerodynamic characteristics in forced oscillation tests. Applying extrapolation results to modeling tends to get better control response compared with test results.

Given the difficulty to acquire aerodynamic characteristics in flight test, it is a good way to get high-

fidelity database through wind tunnel tests covering high angle of attack/sideslip. This paper provides the aerodynamic characteristics for this type of commercial transport aircraft and the database acquired can be used for aerodynamic modeling and flight simulation.

References

[1] Boeing Aviation Safety Group. Statistical summary of commercial jet airplane accidents, worldwide operations, 1959 – 2017. http://www.boeingcom/resources/boeingdotcom/company/about_bca/pdf/statsum.pdf. 2017-10-31.

[2] CEN F, Li Q and Liu ZT, et al. Unsteady aerodynamic test and modeling of civil aircraft under extreme flight conditions. Chinese Journal of Aeronautics, Vol. 41, No.8, p1, 2020.

[3] Shah G H, Cunningham K, Foster J V, et al. Wind-Tunnel Investigation of Commercial Transport Aircraft Aerodynamics at Extreme Flight Conditions. *World Aviation Congress & Exposition.* Warrendale, U.S.A, pp1-8,2002.

5. Contact Author Email Address

Email address: lzbuaa2011@163.com

6. Copyright Statement